CHANNELS
2017, VOL. 11, NO. 6, 517–533
https://doi.org/10.1080/19336950.2017.1369637

Taylor & Francis
Taylor & Francis Group

REVIEW

Mechanisms and models of cardiac sodium channel inactivation

Kathryn E. Mangold, Brittany D. Brumback, Paweorn Angsutararux, Taylor L. Voelker, Wandi Zhu, Po Wei Kang, Jonathan D. Moreno, and Jonathan R. Silva

Department of Biomedical Engineering, Washington University in St. Louis, St. Louis, MO, USA

ABSTRACT

Shortly after cardiac Na^+ channels activate and initiate the action potential, inactivation ensues within milliseconds, attenuating the peak Na^+ current, $I_{Na,}$ and allowing the cell membrane to repolarize. A very limited number of Na^+ channels that do not inactivate carry a persistent I_{Na}, or late I_{Na}. While late I_{Na} is only a small fraction of peak magnitude, it significantly prolongs ventricular action potential duration, which predisposes patients to arrhythmia. Here, we review our current understanding of inactivation mechanisms, their regulation, and how they have been modeled computationally. Based on this body of work, we conclude that inactivation and its connection to late I_{Na} would be best modeled with a "feet-on-the-door" approach where multiple channel components participate in determining inactivation and late I_{Na}. This model reflects experimental findings showing that perturbation of many channel locations can destabilize inactivation and cause pathological late I_{Na}.

ARTICLE HISTORY
Received 10 July 2017
Revised 14 August 2017
Accepted 15 August 2017

KEYWORDS
computational models; inherited arrhythmias; late sodium current; sodium channels

Introduction

In atrial and ventricular myocytes, the Na^+ current (I_{Na}) initiates the action potential (AP) by depolarizing the membrane potential (V_m) from approximately −60 mV to +40 mV. The peak I_{Na} determines the maximum upstroke velocity (dV_m/dt_{max}) and thus the conduction velocity.[1] Within milliseconds (ms), most Na^+ channels inactivate and allow outward K^+ current to repolarize the membrane. The extent of Na^+ channel inactivation and the time to begin recovery from inactivation determines the absolute or effective refractory period (ARP, ERP) where AP initiation is not possible (Fig. 1).[2] Na^+ channel inactivation, recovery from inactivation, and associated deactivation further dictate the relative refractory period (RRP). The RRP describes a time period when sufficient Na^+ channels are available for reactivation and the V_m is further repolarized so that a stronger stimulus may initiate the next AP.[2]

When Na^+ channels do not inactivate completely, a measurable current of less than 0.5% of the peak current persists in the myocyte, known as late or persistent I_{Na}. This current is sustained because it travels through Na^+ channels that do not inactivate completely, so they do not need go through recovery from inactivation. In large mammals, such as dogs and humans, late I_{Na} significantly modulates AP duration (APD) by providing a sustained influx of depolarizing Na^+, which disrupts the "delicate balance" between the inward (primarily L-type Ca^{2+} current) and outward K^+ currents of the AP plateau (Fig. 2).[3,4] Due to the length of the AP plateau, this late component can contribute approximately twice the Na^+ "load" over time compared with the peak current.[5,6] Because the fraction of channels that carry late I_{Na} is small, minute changes to inactivation kinetics at normal heart rate will result in substantial changes to its magnitude, which will affect APD and facilitate (or prevent) anti-arrhythmic activity. APD prolongation based on altered Na^+ channel inactivation and enhanced late I_{Na} is linked to arrhythmia in patients with inherited mutations,[7] heart failure,[8] and myocardial infarction.[9] The purpose of this paper is to review recent and classical findings that shed light on the molecular mechanisms of inactivation and its regulation, how inactivation determines late I_{Na}, and how computational models may capture these mechanisms to connect them to arrhythmia mechanisms.

CONTACT Jonathan R. Silva jonsilva@wustl.edu Biomedical Engineering, Washington University in St. Louis, 1 Brookings Drive, Whitaker Hall, Campus Box 1097, MO 63105, USA.

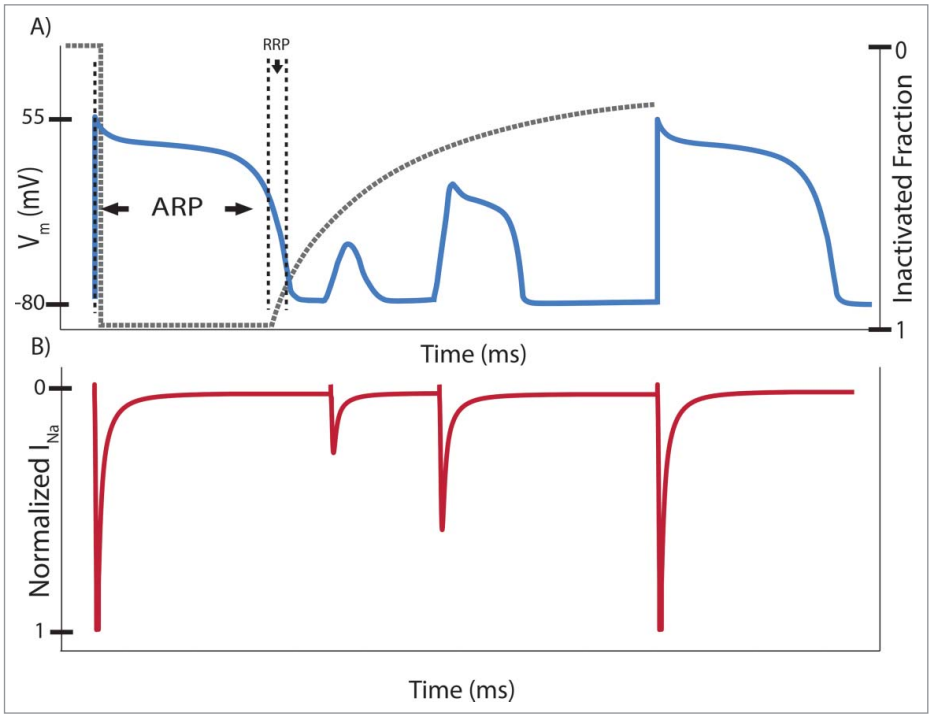

Figure 1. A representative action potential (AP) depicting the corresponding extent of Na^+ channel inactivation (gray dashed line) with labeled absolute (ARP) and relative (RRP) refractory periods. Stimulation immediately after the initial AP results in shortened APs with reduced peak membrane potential (V_m) and peak Na^+ current (I_{Na}). Once the Na^+ channels have recovered sufficiently, they may be reactivated to elicit another full strength AP.

Mechanisms of inactivation

Hodgkin and Huxley clearly recognized the concept of I_{Na} inactivation in 1952 during the first recordings of the axon I_{Na} and modeled it as a monoexponential time and voltage-dependent decay.[10] Work with NaF perfused axons first identified late I_{Na}, which was especially pronounced during depolarizations to elevated potentials, suggesting two components of inactivation.[11,12] Subsequent work identified additional components of inactivation that span many time domains, indicative of multiple relaxations. The fast component became known as fast inactivation (< 10 ms), while intermediate (~100 ms), slow (1 s to 1 min), and ultra-slow (> 1 min) inactivation defined components of inactivation with longer time domains.[13] During an AP, fast inactivation reduces the current to ~0.5% of the peak within millseconds.[6] Cardiac Na^+ channels display reduced slow or ultraslow inactivation compared with neuronal channels, consistent with their essential role in initiating the heartbeat.[14] Over the remainder of the AP, intermediate inactivation will continue to diminish late I_{Na} until Na^+ channels begin to deactivate at negative potentials (below -60 mV).[13] Sustained effort has been applied to measuring inactivation in these different time domains and connecting it to its molecular determinants within the Na^+ channel.

Much of the work to elucidate effects on Na^+ inactivation kinetics was conducted using voltage clamp techniques on Na^+ channels in various expression systems. One must use caution when examining Na^+ kinetic inactivation data because the voltage clamp measurements require adjustments for artifacts, and leak during recording may affect measurement of the late I_{Na}.

Measurement of tetrodotoxin (TTX) sensitive currents is commonly used to correct for membrane leak because it is particularly effective on the late I_{Na} compared with the peak I_{Na}.[15] These experiments work by subtracting currents with TTX added from the control current to isolate the sensitive components. However, the cardiac Na^+ channel ($Na_V1.5$) is not particularly sensitive to TTX, so there are two possibilities to explain this enhanced sensitivity. First, the late I_{Na} may be carried by neuronal Na^+ channels, which are highly TTX sensitive.[16] Another possibility is that Na^+ channels with altered inactivation may inherently be more sensitive to TTX. Further work is needed to distinguish between these two scenarios to precisely

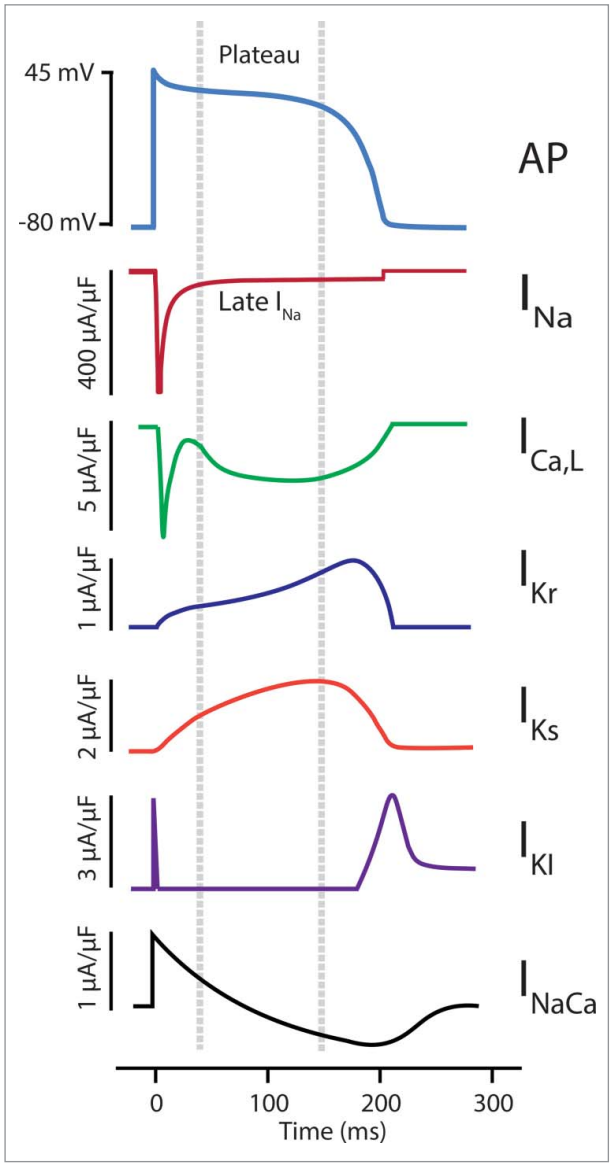

Figure 2. Major currents participating in the action potential (AP) plateau. Late I_{Na} is very effective at modulating the action potential duration (APD) because the other participating currents are relatively small and balance each other out, increasing membrane resistance and reducing the magnitude of $dV_m/dt_{max.}$[142] Representations of the cardiac Na^+ current (I_{Na}), the L-type Ca^{2+} channel ($I_{Ca,L}$), the rapid and slow delayed rectifier K^+ channels (I_{Kr} and I_{Ks}), the inward rectifier K^+ channel (I_{K1}), and current generated by the Na^+-Ca^{2+} exchanger are shown during the AP.

identify which channels are primarily carrying the late I_{Na}.

Further confounding the measurement of Na^+ current, larger cells require a significant amount of time to charge the membrane to a certain potential. This slow charging is problematic when recording rapid Na^+ channel activation kinetics, which are tightly coupled to inactivation kinetics. The cut-open Vaseline gap voltage clamp addresses this difficulty by isolating a patch of large oocytes for recording.[17,18] In smaller cells, such as HEK cells, the patch clamp technique requires compensation for the resistance of the recording electrode and access to the cell, and even then, voltage artifacts are present when recording large currents, making peak current measurements unreliable.[19] Whatever the expression system, it is always difficult to clamp the V_m when examining fast, large inward currents because during a depolarizing pulse the inward I_{Na} is moving the potential in the same direction as the amplifier, creating unstable positive feedback.[20] These challenges in recording I_{Na} are likely responsible for significant variability in published results, particularly regarding the magnitude of the late I_{Na}, which relies on an accurate measure of the peak I_{Na}.

Functional voltage-gated Na^+ channels (Na_v) include nine isoforms that are formed by an α-subunit that comprises four homologous domains (DI-DIV) each with six helical membrane-spanning segments (S1-S6) (Fig. 3).[21,22] In addition to $Na_v1.5$ in cardiac tissue and $Na_v1.4$ in the skeletal muscle, seven other isoforms are expressed in the nervous system.[22] Within each domain, S1-S4 form the voltage sensing domain (VSD), which senses changes in V_m, and S5-S6 form the pore that allows for selective passage of Na^+ ions. In the VSD, S4 contains positive charges, usually arginines, that are thrust outward upon membrane depolarization. These voltage-dependent conformational changes are tightly coupled to the activation, inactivation, deactivation, and recovery from inactivation of the Na^+ channel. Intracellular linkers attach each domain to the next, connect the channel to the cytoskeleton and intracellular signaling pathways, and regulate channel gating. The C-terminus is composed of a structured proximal portion and unstructured distal portion.[23,24] The structured portion has six α-helices that form an EF hand-like structure (α helices 1–5) and an IQ motif which surprisingly has higher calcium binding affinity than the EF-hand (α helix 6).[24]

Clever experiments with intracellularly applied pronase, a non-specific protease, demonstrated that the fast inactivation gate is located on the intracellular face of the Na^+ channel.[25] Intracellular pronase perfusion removed inactivation while preserving I_{Na} activation and deactivation. After the Na^+ channel was cloned, further work showed that

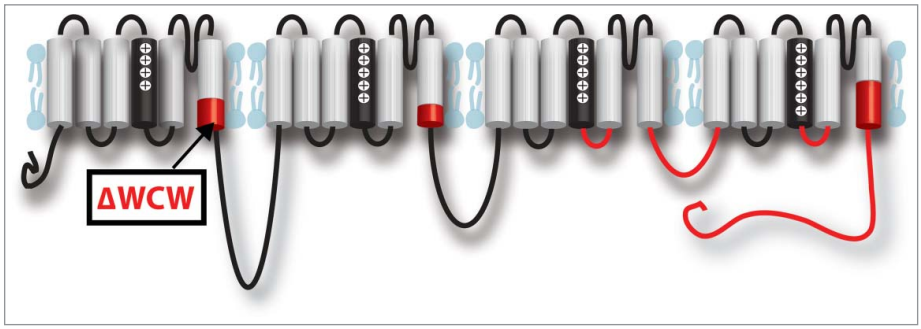

Figure 3. Structures involved in inactivation within the $Na_v1.5$ α-subunit. Structures colored in red significantly affect fast inactivation. From N-terminal to C-terminal, the intracellular end of DI S6 segment (ΔWCW window),[45,47] intracellular end of DII S6 segment,[45] DIII S4-S5 linker,[38,39,42] DIII-DIV linker,[25-33] DIV S4-S5 linker,[40-42] lower half of DIV S6 segment,[44,47] and C-terminus.[23,48-51,53]

antibodies,[26] cleavage, [27] and additions[28] to the intracellular DIII-DIV linker were sufficient to inhibit inactivation, and a primarily hydrophobic motif identified through site-directed mutagenesis on the linker is crucial for successful fast inactivation (IFMT): I-1488, F-1489, M-1490, and T-1491.[29-31] Sulfhydryl accessibility studies showed that F1489 becomes inaccessible during fast inactivation,[32] and the interaction between the channel and the motif is hydrophobic.[30] Smaller residues containing glycine and proline provide the flexibility for a "hinged lid" or "chain" that allows IFMT to occlude the channel.[33] How and where the DIII-DIV linker and these primarily hydrophobic residues interact with the rest of the channel has remained a key topic of research for many years.

Gating current recordings have yielded critical insights into the DIII-DIV linker interactions with the VSDs. The gating current arises from the rapid movement of the S4 charges within membrane, which enables their detection.[34] Early gating current recordings showed that two-thirds of the gating charge, which is measured as the integral over time of the gating current, is immobilized when fast inactivation occurs, suggesting a connection between the VSDs and inactivation.[35] The application of voltage clamp fluorometry (VCF) to Na_V channels has allowed monitoring of each VSD individually, rather than the summation of their movement reported by the gating current.[36,37] During VCF experiments, a fluorophore is attached to the S4 segment of a domain. When a potential is applied, S4 displacement results in a change of environment around the fluorophore, which is detected as a deflection in the fluorescence intensity with a high dynamic range amplifier. Using VCF, Cha et al. showed that the voltage-dependent kinetics of the DIII and DIV VSDs are modulated by inactivation.[37]

Site-directed mutagenesis has provided additional insights, showing inactivation can also be modulated by the S4-S5 linkers of DIII and DIV. A conserved alanine on the $Na_v1.2$ DIII S4-S5 linker severely disrupted inactivation when it was mutated to glutamine and was proposed to serve as a hydrophobic "docking" site for the IFMT motif.[38] Further work showed that some patients with long QT type 3 syndrome, which increases late I_{Na}, carry a mutation to a homologous conserved alanine within this linker in $Na_v1.5$.[39] The DIV S4-S5 has also been shown to significantly affect inactivation and suggested as a potential "docking" site for the inactivation gate.[40,41] Confoundingly, accessibility studies with $Na_v1.4$ showed that both the DIII S4-S5 and DIV S4-S5 linkers remain accessible when channels are inactivated.[40,42]

Mutagenesis work also aided in demonstrating that the S6 segments of DI, DII, and DIV modulate fast inactivation. An alanine-mutagenesis study showed that mutations in the center[43] and in intracellular[44] end of DIV S6 segment in $Na_v1.2$ inhibited inactivation. Double mutations within the center and intracellular end of DIV S6 exhibit more inactivation inhibition, but the IFMT does not likely interact with the S6 segments as changing the hydrophobic characteristics of the mutations did not affect the phenotype. Mutations in the intracellular end of DIS6 and DIIS6 in $Na_v1.2$ also inhibit fast inactivation[45] while no mutations were found in DIIIS6.[46] Finally, work with tryptophan scanning mutations in $Na_v1.4$ in the DI and DIV S6 segments identified the "WCW" window located on the intracellular DI S6 segment that impairs fast inactivation.[47]

The C-terminus also plays an important role in modulating Na^+ channel inactivation.[48] Generally,

each Na^+ channel homolog has distinct fast inactivation kinetics. For example, $Na_v1.5$ fast inactivation is slower than $Na_v1.4$ due to differences in amino acid sequences in the C-terminal domains.[49] In addition, swapping C-terminal domains between $Na_v1.5$ and $Na_v1.2$ causes a shift in voltage-dependent steady-state inactivation toward the potential of the original isoform.[50] Mutations in the C-terminal domain have also been shown to disrupt fast inactivation and cause cardiac arrhythmias such as long QT syndrome.[51,52]

Work with truncated C-terminal mutants identified the importance of the sixth helix and the distal portion in inactivation regulation. When just the distal, unstructured portion of the C-terminus was removed, inactivation was not affected; however, when the distal portion along with the sixth helix were removed, inactivation was inhibited.[23] Pull-down assays confirmed that the DIII-DIV linker interacts with the sixth helix and distal portion of the C-terminus, and mutagenesis showed that the interaction likely stabilizes the inactivated state.[53]

Toward the goal of understanding how various channel domains regulate Na_V channel gating, recent VCF experiments have shown that DIV-VSD translocation serves as a rate limiting step to initiate fast inactivation.[54] Later results also showed that the VSDs of DI-DIII are also likely involved with slower components of inactivation.[55,56] Work with inactivation deficient mutations shows that the DIII-VSD also participates in fast inactivation but only after pulses with durations of 100s of ms.[57,58] Together these results suggest a model where the hydrophobic IFM sequence of DIII-DIV linker quickly associates with DIV-VSD to initiate fast inactivation (Fig. 4). After about 100 ms, the DIII-DIV linker then associates with the DIII-VSD and supports its activated conformation. This late association will stabilize the inactivated state, causing a reduction in late I_{Na}.

The above results show that Na_v inactivation is a complex phenomenon that involves locations across the α-subunit. The various structures participating inactivation are highlighted in Fig. 3. The primary structure of fast inactivation is the DIII-DIV linker, which physically occludes the intracellular mouth of the channel. The linker's IFMT motif mediates successful occlusion through hydrophobic interactions between the linker and the channel. While the DIII-DIV linker occludes the pore, various structures across the α-subunit modulate the extent of inactivation and

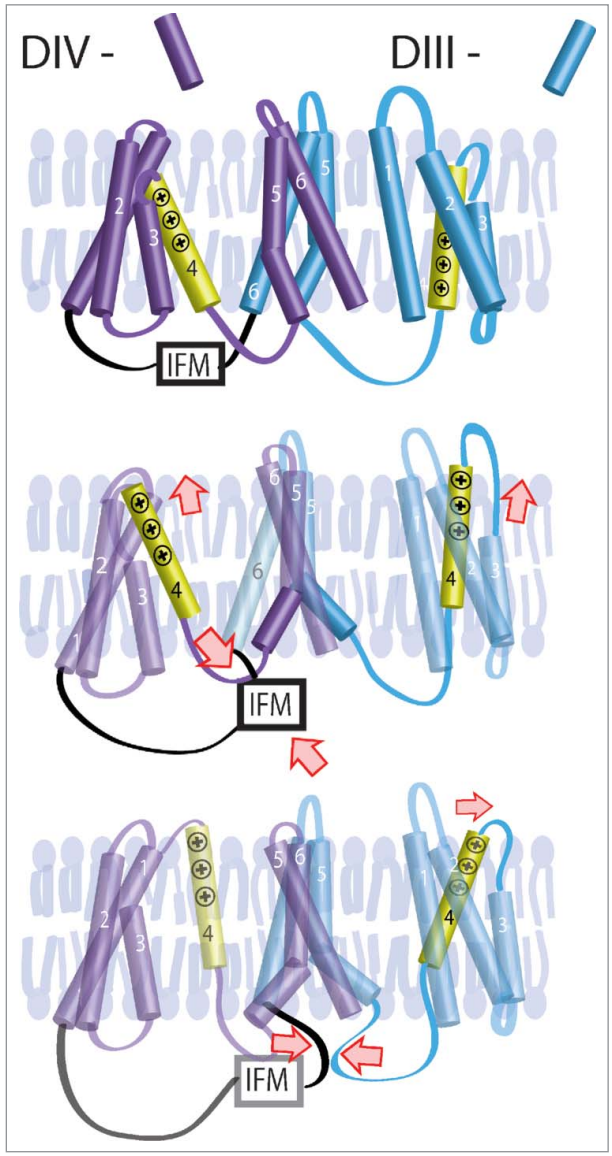

Figure 4. Inactivation is significantly determined by the DIII and DIV VSDs.[57] After channel activation, IFM associates with the DIV-VSD to control inactivation onset. After ~100 ms, the IFM also associates with the DIII-VSD, supporting its activated conformation. Only after the IFM dissociates from the DIII and DIV VSDs. © Hsu et al. Adapted by permission of the CC BY 4.0 license. Permission to reuse must be obtained from the rightsholder.[57].

therefore late I_{Na}: the DIII and DIV VSDs, the DI and DIV S6 segments, and the C-terminal domain.

Regulation of inactivation by accessory subunits

Na^+ channel inactivation is not only modulated by α-subunit structures, but also by external factors, such as accessory subunits and the external environment. These may regulate inactivation alone or in combination with the α-subunit.

The most studied interacting partners of the Na_v α-subunit are the β-subunits, which are found in complex with the Na_V channel α-subunit after purification. There are five types of voltage-gated Na^+ channel β-subunits (β1–4 and β1b, a splice variant of β1).[59-63] All β-subunits, with the exception of β1b, are composed of an extracellular immunoglobulin domain, a transmembrane segment, and an intracellular C-terminus.[64] β1b is missing the transmembrane segment.[65] The β1 and β3 subunits interact noncovalently with α-subunit[62,66] while β2 and β4 covalently bind to α subunit through disulfide bonds.[64,67] The expression level for each β-subunit is tissue and cell-specific with varying patterns over the course of development.[68-70] While each β-subunit paralog causes an increase in channel expression, the regulation of biophysical properties including voltage-dependence of activation and inactivation, rate of inactivation, recovery from inactivation, and magnitude of persistent and resurgent I_{Na} are unique.[63,64,71-74] Very recent structures of the $Na_v1.4$-β1 complex in the electric eel show that the immunoglobulin domain of the β1 subunit interacts with the extracellular loops of the DI and DIV pore domain while the transmembrane domain interacts with the DIII-VSD.[75] This structure serves as a basis for determining how β1-subunit interactions with the α-subunit mediate biophysical property regulation.[75] However, the interactions revealed by this structure failed to elucidate how β1 regulates channel inactivation, suggesting that kinetic data are essential for fully understanding regulation of the channel by β subunits. Concurrently, we used the VCF technique to assess the modulation of Na^+ channel VSD conformations by β1 and β3 during gating.[76] The β1 subunit caused the DIV-VSD to activate at higher potentials. Because the DIV-VSD activation has been connected to fast inactivation onset, modulation of the DIV-VSD by β1 explains why it affects channel inactivation. Intriguingly, despite the sequence homology between the β1 and β3 subunit, the β3 subunit controls the DIII-VSD along with the DIV-VSD. This additional interaction with the DIII-VSD allows β3 to alter both current activation and inactivation kinetics.

The regulatory effects of β-subunits on Na^+ channel inactivation are system and cell type specific. As a result, there are many conflicting results regarding the magnitude and direction of the inactivation shifts by different β-subunits.[77] These discrepancies likely reflect the fact that α-subunits interact not only with β-subunits but also with many other modulating proteins that altogether form the macromolecular Na^+ channel complex.[78]

Multiple Brugada syndrome-associated mutations have been identified in *SCN1B* (encoding for β1 subunit, E87Q, and β1b subunit H162P, W179X, R214Q), *SCN2B* (encoding for β2 subunit, D211G), and *SCN3B* (encoding for β3 subunit, L10P, V110I).[65] Patients with the Brugada syndrome often have reduced I_{Na}, which can lead to arrhythmia through a variety of mechanisms.[79] These mutations can cause I_{Na} reduction by lowering I_{Na} density, due to a hyperpolarizing shift in steady-state inactivation or altering inactivation onset and recovery rates.[65] In contrast, mutations in β4 (L179F) and β1B (P213T) that are associated with long QT syndrome cause a depolarizing shift in steady-state inactivation.[80] These mutations lead to increased channel availability and elevated late I_{Na}, which prolongs the ventricular AP and therefore the QT interval.

Work with various Na_v β-subunit knockout mouse models have also revealed associated cardiac abnormalities. The *Scn1b* null mouse model exhibited increased APD and prolonged QT intervals with transient and persistent peak I_{Na}.[81] *Scn2b* null mice showed reduced I_{Na} density with slower conduction velocity and repolarization in the right ventricular outflow tract, leading to ventricular arrhythmia.[82] The *Scn3b* null mice also displayed cardiac abnormalities such as reduced peak I_{Na} and altered sinoatrial node recovery.[83,84] Together, these findings demonstrate the physiologic relevance of β-subunits on the regulation of Na^+ channel biophysical properties including inactivation, reactivation, and recovery.

Other than Na_V β-subunits, the Na_V α-subunit is associated with plethora of auxiliary subunits for additional regulatory effects. One prominent auxiliary subunit well known to bind the Na_V α-subunit C-terminal domain is calmodulin (CaM).[85] CaM is a bi-lobed, ~17 kDa protein which functions as a ubiquitous Ca^{2+} sensing protein.[86] Therefore, CaM association to Na_V channels may endow the channels with Ca^{2+} regulation. The leading hypothesis concerning the nature of Ca^{2+} regulation of Na_V channels involves shifts in the steady-state inactivation, thus tuning Na^+ channel availability depending on levels of intracellular Ca^{2+}.[87] Despite extensive characterization, Ca^{2+} regulation of Na_V

channels appear to be idiosyncratic and isoform specific.[88-91] Elevated intracellular Ca^{2+} has been reported to induce a depolarizing shift in the steady-state inactivation of $Na_V1.5$,[89,92-94] but other studies reported no shift in the steady-state inactivation of $Na_V1.5$ in response to elevated intracellular Ca^{2+}.[88,91] Furthermore, elevated intracellular Ca^{2+} levels were reported to induce a hyperpolarizing shift in the steady-state inactivation in $Na_V1.4$.[88] Just as the functional effect of Ca^{2+} on Na_V channel is controversial, the mechanism behind Ca^{2+} regulation of Na_V channels is also debated. Ca^{2+} has been proposed to directly bind the C-terminal domain of Na_V α-subunit to exert regulatory effect independent of CaM.[92] Other models proposed that upon Ca^{2+} binding, Ca^{2+}/CaM interacts with DIII-DIV linker to induce regulation of steady-state inactivation.[95] Overall, the question of whether Ca^{2+} itself, or the ion in complex with CaM, regulates Na^+ channel inactivation remains a controversial topic.

A group of four proteins, fibroblast growth factors (FGF 11–14), also referred to as fibroblast growth homologous factors (FHFs 1–4), interact with the C-terminal domain in the Ca^{2+}-CaM complex.[96,97] FHFs are differentially expressed in various tissues and lack the N-terminal signal sequence, causing them to remain in the cytoplasm and allowing them to regulate Na_V and Ca^{2+} channels.[78,96,98] Work with FHF1B demonstrated that its interaction with the C-terminal domain of $Na_v1.5$ produces a hyperpolarizing shift in steady-state inactivation, and the mutation D1790G, which is already associated with the long QT type 3 syndrome, interrupts interaction between FHF1B and the C-terminus.[99] In addition, a mutation in $Na_v1.5$ that interrupts FHF binding to the C-terminal domain displayed slowed inactivation kinetics, resulting in increased late I_{Na} and prolonged APD.[100]

As can be appreciated from the results discussed above, many different accessory subunits can regulate Na_V channel inactivation and disruption of this regulation leads to deadly arrhythmias. Fig. 5 presents a pictorial representation of accessory subunits involved in modulating inactivation. A precise understanding of how accessory subunits regulate inactivation will prove challenging because the channels are composed of subunits that interact with each other. However, this work will lead to an improved understanding of diseased states and potentially new therapeutic routes.

Environmental regulation of inactivation

Acidosis and febrile states are both environmental factors that alter cardiac electrical activity by shifting Na^+ channel inactivation properties. These effects are often exacerbated by underlying $Na_V1.5$ mutations, which can lead to life-threatening phenotypes.[101-103]

In physiologic conditions, human arterial blood pH is maintained at approximately 7.4.[101] If pH drops just 0.05 units, protein function may be altered,[101] and pH below 6.95 results in deleterious effects on protein function in cardiomyocytes.[101] During cardiac ischemia, myocytes experience pH as low as 5.9. Reduced extracellular pH due to arterial blood acidosis has been shown to reversibly destabilize the fast-inactivated state in wild-type $Na_V1.5$ channels, leading to increased window current and increased late I_{Na}, and to destabilize the slow inactivated state.[101,104] Specifically, proton block of wild-type channels accelerates the recovery from open state fast inactivation and delays its onset.[101,102] *In silico* studies have demonstrated that these effects on wild-type channels can be sufficient to prolong the AP and decrease its maximum upstroke

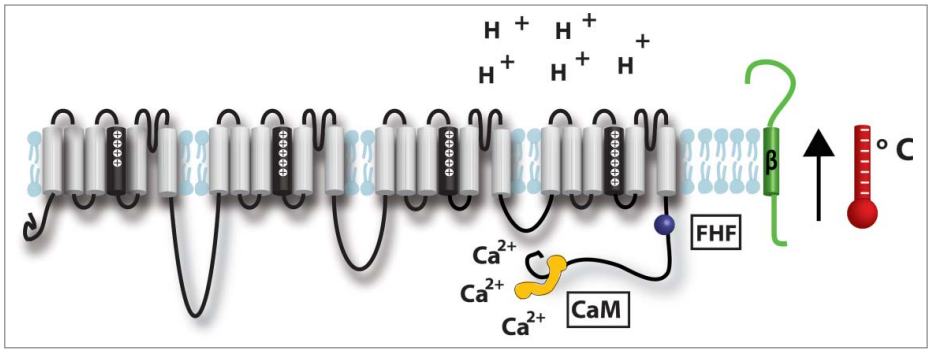

Figure 5. Accessory subunits involved in modulating $Na_v1.5$ inactivation: β-subunit (green),[59-74,80,81,83,84,143-145], fibroblast growth homologous factors (FHFs) (purple),[96,97,99,121,122] and the CaM/Ca^{2+} complex (yellow).[24,89,91,95-97,146-150] Environmental factors including extracellular pH,[101,102,104,105,110] and temperature[103,112-120,122] may also modulate Na^+ channel inactivation.

velocity, which affects conduction velocity.[1,103,105] Both AP effects predispose patients to arrhythmia.[103,106] The conclusions from these modeling studies have been strengthened by multiple reports of Brugada syndrome phenocopy induced by acidosis.[107,108] When the patient's blood pH returned to physiologic conditions and electrolytes were balanced, the Brugada syndrome characteristic ECG was no longer present.[108]

Certain $Na_v1.5$ mutations that cause long QT or Brugada syndromes result in APs that are more sensitive to acidosis.[109,110] Studies have shown that a low pH environment in combination with these underlying mutations exacerbates the electrical abnormalities in individuals.[103] For example, decreased extracellular pH paired with E1784K, the most common *SCN5A* (encoding for $Na_v1.5$) mutant linked to both Brugada syndrome and LQT3, leads to significantly larger increases in late I_{Na} due to more severe alterations to the channel inactivation.[109] Other groups have shown that certain long QT type 3 syndrome mutations are more sensitive to intracellular acidosis than others.[111]

Another environmental factor modulating the Na^+ channel is body temperature. In healthy humans, without underlying mutations in $Na_v1.5$ or other conditions, temperature-dependent cardiac abnormalities may occur in extreme hyperthermia but seldom when they experience a mild fever.[112,113] In contrast, individuals with Na_V channel mutations are more sensitive to core body temperature fluctuations with their susceptibility to arrhythmia being dependent on the mutation that they carry.[110,114,115] Several studies have shown that hyperthermia has detrimental effects on asymptomatic Brugada syndrome patients causing Brugada syndrome ECG patterns to be unmasked under febrile conditions and remain unmasked when core body temperature is restored.[116,117] Other clinical studies have presented in patients who only possessed a Brugada syndrome ECG pattern while in the febrile state.[118,119] While the mechanisms responsible for this phenomenon are still under investigation, it is known that elevated temperature increases the rate of fast inactivation recovery and onset for wild-type Na^+ channels, which leads to decreased late I_{Na}.[114,116]

The T1620M missense mutation found in *SCN5A* alters the temperature sensitivity of Na^+ channel fast inactivation in patients with Brugada syndrome. As temperatures increase toward the physiologic range, these mutant cardiac Na^+ channels demonstrate slower recovery from inactivation, leading to further loss of function of I_{Na}.[115] Q10 extrapolation results suggest that febrile states would elicit worsening of this mutant's inactivation properties and become more arrhythmogenic.

However, studies of different *SCN5A* mutations suggest that febrile states do not worsen these mutation effects.[116] Keller et al. demonstrated patients who had fever-induced type 1 Brugada syndrome and fever-induced arrhythmias also possessed mutations, such as R535X and L325R, which result in severe to absolute loss of I_{Na} at physiologic temperature. Thus, the study suggested that fever could not make the channel function any worse, and fever did not significantly worsen the biophysical changes to the channel. Therefore, the authors hypothesized that in heterozygous patients, possessing both wild-type and mutated Na^+ channels, the effect of temperature accelerating the inactivation of the wild-type channels, not the effect on mutant channels, is responsible for altering the delicate balance of depolarization and repolarization currents and thus may lead to fever-induced arrhythmias. This hypothesis is supported by Gima and Rudy's modeling study which demonstrated that accelerated inactivation, a consequence of fever, of the T1620M $Na_V1.5$ mutant channel causes a Brugada syndrome pseudo ECG phenotype through the resultant decrease in late I_{Na} combined with the already reduced peak I_{Na} from the mutant channel.[116,120] Regardless of whether a *SCN5A* mutant makes a channel more sensitive to temperature effects, it is evident that febrile temperatures in combination with mutations increase the risk of fever-induced arrhythmias, particularly from asymptomatic Brugada syndrome patients.

Temperature-dependent cardiac electrical abnormalities are not limited to mutations in *SCN5A*. A recent study identified FHF2, a member of the FHF protein family known to modulate voltage-gated Na^+ channel inactivation as previously discussed, as a key regulator of myocardial excitability that prevents conduction failure in mouse heart under hyperthermic conditions.[121,122] Loss of FHF2, accelerates the rate of both open state and closed state inactivation of the Na^+ channel. This change becomes functionally relevant under febrile temperatures when temperature dependence increases the inactivation rate, resulting in severely suppressed I_{Na} and ultimately conduction failure.

Environmental factors, such as acidosis and temperature, have significant effects on Na^+ channel

inactivation and are depicted in Fig. 5. Patients already harboring mutations for cardiac abnormalities, such as long QT or Brugada syndromes, often exhibit aggravated symptoms when subject to acidosis or hyperthermia. Understanding how environmental factors combine with channel structure to disrupt inactivation may lead to better clinical strategies for preventing these pathological situations.

Models of inactivation

Modeling of Na_V channel inactivation began with Hodgkin and Huxley's work in 1952 with the squid giant axon.[10] When analyzing the Na^+ conductance curves, they inferred that Na^+ conductance could be represented by a product of probabilistic gates, which required residence in a permissive conformation for conduction to occur. These gates could regulate either activation, with initial and maximum values of zero and one, respectively, or inactivation with hyperpolarized and depolarized values of one and zero, respectively. Hodgkin and Huxley found that the product of 3 activation gates and one inactivation gate adequately described the conductance curves. Under this model, 3 of 4 domains had an activation gate that must open for conduction to occur, and one domain had a gate that would close to mimic inactivation. Because conductance was represented as product of activation and inactivation, the activation and inactivation processes were assumed to be independent. While we now know that activation and inactivation are instead coupled, this idea that three domains primarily control activation and one primarily controls inactivation is still useful.[123] Chandler and Meves' later work in 1970 suggested multiple components of Hodgkin and Huxley's inactivation gate.[11,12] Their work with NaF perfused squid axons demonstrated that large depolarizations resulted in less steady-state inactivation and thus maintained late I_{Na}. They suggested amending Hodgkin and Huxley's single inactivation gate model to an inactivation gate with two components to account for transient peak in Na^+ channel conductance upon activation followed by sustained late conductance. Further, they suggested that the Na^+ channel may have two open states with a higher and lower probability of conductance.

As mentioned previously, the early pronase experiments, which localized inactivation to the intracellular part of the channel, suggested the use of a "inactivation particle" that would physically occlude the channel.[25] Several years later, a study on gating charge movement suggested that inactivation immobilizes two thirds of the gating charge, but the inactivation process itself is not associated with any gating current.[35,124] Because a voltage-dependent process produces an associated gating current, and inactivation lacks this associated gating current, Armstrong and Bezanilla concluded that inactivation must be a voltage-independent process, which is contrast to Hodgkin and Huxley's original theory.[35] Additionally, because the fast time component of activation moves more than half of the total gating charge, and inactivation immobilizes two thirds of the total gating charge, Armstrong and Bezanilla deduced that inactivation must immobilize gating charge that was moved by channel activation. Thus, the processes of activation and inactivation are coupled. Combining these results led to the "ball and chain model" of inactivation. This model proposes that a "ball," tethered to the intracellular channel by a polypeptide "chain," occludes the mouth of the channel to bring about fast inactivation only after activation.[35]

The discovery of the IFMT motif on the DIII-DIV linker crucial for successful fast inactivation suggested that the "ball and chain" model of inactivation needed updating. First, the determination that a primarily hydrophobic IFM motif controls successful inactivation demonstrates that hydrophobic interactions occlude the pore rather than the proposed electrostatic attraction between the inactivation particle and channel.[29] Second, structural studies determined that the middle of the DIII-DIV linker has an α-helical structure containing the IFMT motif, which is flanked by glycines N-terminally and prolines C-terminally.[29,31] This structure and residue sequence suggests that the DIII-DIV linker functions as a "hinged lid" to occlude the pore instead of the "loosely tethered" blocking ball. In the "hinged lid" model of inactivation the DIII-DIV linker closes in on its "hinges," composed of glycine or proline, to block the intracellular mouth of the channel.[29] West further suggests that the IFM sequence serves as a hydrophobic "latch" to keep the lid closed.

Data collected from single-channel recordings in the giant squid axon in combination with the gating charge data required Markov type models that include state-dependent transitions to simulate their results.[125,126] Experimental recordings kinetics confirm that transitions between hypothetical states can be made sufficiently fast for a valid state-dependent representation of Na^+

channel processes such as inactivation.[127] Markov models are also more generalizable and allow for activation and inactivation to be modeled as a coupled process and may be reduced to the Hodgkin-Huxley formalism if desired for simplicity.[128] The earliest models incorporating inactivation included 3 states: an open, closed, and inactivated state.[125,126]

Vandenberg and Bezanilla in 1991 created a Markov-type model of I_{Na} with data from single-channel recordings in the giant squid axon.[129] The recordings showed that channels not only inactivate from the open state but also from the closed state as well. In addition to adding transitions between inactivated, closed and open states, the models incorporated reversible inactivation along multiple closed states for better fits to recordings. Rate constants were obtained from the single-channel recordings using maximum likelihood analysis and scaled up to yield macroscopic gating and channel currents.

In the spirit of Chandler and Meves' observations of two types of Na^+ channel conductance in 1970, Keynes detailed a "mode switching hypothesis" to explain inactivation.[130] This hypothesis included two open states: one initial open state with a high probability of opening and a second open state with a lower probability of opening. He proposed that "modulation of energy wells" rather than movement of an inactivating particle to block the channel pore would theoretically explain the transition from the first open state to the second. Practically, he suggested that "voltage sensor S4d" drives the channel to a second open state through "lateral movement" or deionization of charge. This theory is in accordance with the finding that fluorescence signals near the DIV-VSD are associated with the slow component of gating and appear after signals associated with the faster component of gating (DI-DIII).[131] Keynes defended his "mode switching" hypothesis based on new evidence suggesting Na^+ channels maintain conductance even during inactivation.[132] He also cited single channel recordings from Vandenberg and Bezanilla 1991 to support his theory.[129] The recordings depict a channel with multiple openings initially after activation, but with time the number of openings would decrease. He thought this channel behavior would be best captured by a model with two open states. Later Keynes (1998) updated his model to include recent mutation studies suggesting that DIV S4 movement controls the onset of fast inactivation, or in other words, the initial transition from the first to the second open state.[133] He further proposed that the hydration of the Na^+ channel would control the transition from the second open state into an inactivated state. He finally suggested that the DIII-DIV linker controls the "hydration equilibrium" that eventually closes the channel.

Finally, the discovery of inherited long QT syndrome mutations that impair Na^+ channel inactivation informed a new generation of models. In 1999, Clancy and Rudy simulated the ΔKPQ channel using a Markov type model.[134] This mutation is in the DIII-DIV linker, and single channel recordings showed that the channel could enter a bursting state where inactivation fails to inactivate. To model this behavior, a six-state wild-type model was extended to include a "burst mode" that represents channel that fail to inactivate. Once a channel entered the "burst mode," the channel lost its access to inactivation until it exited, producing late $I_{Na.}$. The model successfully recapitulated single channel data and reproduced the cell level behavior producing a prolonged APD, consistent with the long QT phenotype.

Toward molecularly detailed models of inactivation

While recent models are capable of recapitulating single channel behavior, they conflict with experimental evidence that shows that many different channel locales contribute to channel inactivation. Specifically, the models suggest that a specific, identifiable switch causes the channel to enter a mode where inactivation is impossible.

In contrast, the experimental findings detailed above suggest that several different channel domains contribute to inactivation during an AP. During the first few ms the DIV-VSD activates, enabling fast inactivation, which closes most of the channels. Subsequently, at least the DIII-VSD and C-terminal domain stabilize the inactivated conformation, causing more channels to occupy a non-conducting state. This mechanism is reminiscent of the "foot-on-the-door" mechanism used to explain Cd^{2+} ions promoting closure of the ultraslow inactivation gate in $Na_v1.4$.[135] However, instead of a single foot on the door, there are at least two feet, the C-terminal domain and the DIII-VSD that stabilize the inactivated state. Fig. 6 compares the traditional and the "feet-on-the-door" models of inactivation. The traditional model suggests that a switch induces the channel to enter a mode

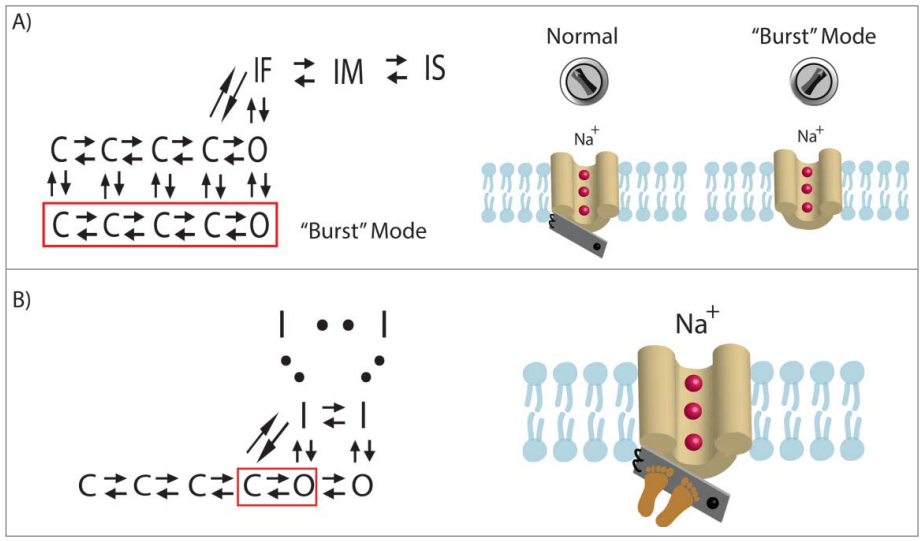

Figure 6. A comparison of the traditional and "feet-on-the-door" models. (A) In the traditional model, a switch induces the channel to enter a separate "burst" mode where inactivation is not possible. Once in the "burst" mode, the channel may not transition back to normal gating. The Markov type representation of this separate "bursting" mode is section of closed and open states (outlined in red) with rate parameters that prescribe periodic "bursting."[134] (B) The "feet-on-the-door" model of Na^+ channel inactivation maintains that the IFM motif on the DIII-DIV linker is key for successful fast inactivation and that the C-terminal domain and the DIII-VSD keep the inactivation "door" closed. The corresponding Markov type representation includes a series of inactivated states with increasing stability. Higher stabilization allows the channel to occupy a deeper inactivated state where transitioning back to open and closed states is unlikely. Two open states are included where the rightmost open state has the higher open probability compared with left open state.[130] Bursting behavior would be observed when channels occupy the left open and closed states (outlined in red). The extent of stabilization of inactivation determines the magnitude of late I_{Na}.

where inactivation is not possible while the "feet-on-the-door" model suggests that increased late I_{Na} is a consequence of one of the feet failing to stabilize the inactivated state. Because this model suggests that disruption of many different stabilizing events can cause increased late I_{Na}, it explains why mutations in various channel locations can augment late I_{Na}.

The creation of computational models that explicitly represent the molecular determinants of inactivation will not be trivial because each of these components cooperatively interact with each other, significantly increasing model complexity. Recent developments in channel optimization algorithms may be helpful in this effort.[136,137] One potential approach to create a Markov type model with a large training set is to use state-mutating optimization routine. Instead of fixing the model topology which may overcomplicate the optimization, the routine identifies the optimal number of states along the corresponding rate parameters.[136] Using the matrix exponential to compute cost saves time compared with using standard ODE solvers during the optimization.[137] This expedited cost computation allows for larger sets of training data to be recapitulated in a reasonable amount of time.

While the challenge of creating molecularly based models of inactivation is not insignificant, there are many potential rewards. Because computational models of channels are readily incorporated into multiscale cell and tissue models,[136,138] this approach could be used to identify how inactivation should be targeted therapeutically to stabilize excitation at the tissue level to prevent arrhythmia. As additional structural data emerges, including the Cryo-EM structure of a mammalian Na_V channel,[139] conformational data from fluorescence experiments,[140] and even NMR data showing channel dynamics,[141] these models will only improve, provided that the computational approaches needed to incorporate this type of information into the models continue to be developed in parallel.

Disclosure of potential conflicts of interest

No potential conflicts of interest were disclosed.

Funding

This work was supported by National Institutes of Health under grant R01-HL136553 (JS) and grant T32-HL134635 (KM), and the American Heart Association under grant 15PRE25080073 (WZ).

References

[1] Shaw RM, Rudy Y. Ionic Mechanisms of Propagation in Cardiac Tissue. Circ Res. 1997;81:727 LP-741. doi:10.1161/01.RES.81.5.727. PMID:9351447

[2] Jaye DA, Xiao Y-F, Sigg DC. Basic Cardiac Electrophysiology: Excitable Membranes BT – Cardiac Electrophysiology Methods and Models. In: Sigg DC, Iaizzo PA, Xiao Y-F, He B, editors. Boston (MA): Springer US; 2010. P. 41-51. doi:10.1007/978-1-4419-6658-2_2

[3] Hund TJ, Rudy Y. Rate dependence and regulation of action potential and calcium transient in a canine cardiac ventricular cell model. Circulation. 2004;110:3168-74. doi:10.1161/01.CIR.0000147231.69595.D3. PMID:15505083

[4] O'Hara T, Virág L, Varró A, Rudy Y. Simulation of the Undiseased Human Cardiac Ventricular Action Potential: Model Formulation and Experimental Validation. PLOS Comput Biol. 2011;7:e1002061. doi:10.1371/journal.pcbi.1002061. PMID:21637795

[5] Makielski JC. "Late sodium current: a mechanism for angina, heart failure, and arrhythmia." J Cardiovasc Pharmacol. 2009;54:279-86. doi:10.1097/FJC.0b013e3181a1b9e7. PMID:19333133

[6] Makielski JC, Farley AL. Na+ Current in Human Ventricle: Implications for Sodium Loading and Homeostasis. J Cardiovasc Electrophysiol. 2006;17:S15—20. doi:10.1111/j.1540-8167.2006.00380.x. PMID:16686671

[7] Dumaine R, Wang Q, Keating MT, Hartmann HA, Schwartz PJ, Brown AM, Kirsch GE. Multiple mechanisms of Na+ channel–linked long-QT syndrome. Circ Res. 1996;78:916-24. doi:10.1161/01.RES.78.5.916. PMID:8620612

[8] Maltsev VA, Undrovinas A. Late sodium current in failing heart: Friend or foe? Prog Biophys Mol Biol. 2008;96:421-51. doi:10.1016/j.pbiomolbio.2007.07.010. PMID:17854868

[9] Huang B, El-Sherif T, Gidh-Jain M, Qin D, El-Sherif N. Alterations of sodium channel kinetics and gene expression in the postinfarction remodeled myocardium. J Cardiovasc Electrophysiol. 2001;12:218-25. doi:10.1046/j.1540-8167.2001.00218.x. PMID:11232622

[10] Hodgkin AL, Huxley AF. A quantitative description of membrane current and its application to conduction and excitation in nerve. J Physiol. 1952;117:500-44. doi:10.1113/jphysiol.1952.sp004764. PMID:12991237

[11] Chandler WK, Meves H. Sodium and potassium currents in squid axons perfused with fluoride solutions. J Physiol. 1970;211:623-52. doi:10.1113/jphysiol.1970.sp009297. PMID:5501055

[12] Chandler WK, Meves H. Rate constants associated with changes in sodium conductance in axons perfused with sodium fluoride. J Physiol. 1970;211:679-705. doi:10.1113/jphysiol.1970.sp009299. PMID:5501057

[13] Silva J. Slow Inactivation of Na+ Channels BT – Voltage Gated Sodium Channels. In: Ruben PC, editor. Berlin (Heidelberg): Springer Berlin Heidelberg; 2014. p. 33-49. doi:10.1007/978-3-642-41588-3_3

[14] Richmond JE, Featherstone DE, Hartmann H a, Ruben PC. Slow inactivation in human cardiac sodium channels. Biophys J. 1998;74:2945-52. doi:10.1016/S0006-3495(98)78001-4. PMID:9635748

[15] Biet M, Barajas-Martinez H, Ton A-T, Delabre J-F, Morin N, Dumaine R. About half of the late sodium current in cardiac myocytes from dog ventricle is due to non-cardiac-type Na(+) channels. J Mol Cell Cardiol. 2012;53:593-8. doi:10.1016/j.yjmcc.2012.06.012. PMID:22759452

[16] Biet M, Morin N, Lessard-Beaudoin M, Graham RK, Duss S, Gagne J, Sanon NT, Carmant L, Dumaine R. Prolongation of action potential duration and QT interval during epilepsy linked to increased contribution of neuronal sodium channels to cardiac late Na+ current: potential mechanism for sudden death in epilepsy. Circ Arrhythm Electrophysiol. 2015;8:912-20. doi:10.1161/CIRCEP.114.002693. PMID:26067667

[17] Stefani E, Bezanilla F. Cut-open oocyte voltage-clamp technique. Methods Enzymol. 1998;293:300-18. doi:10.1016/S0076-6879(98)93020-8. PMID:9711615

[18] Rudokas MW, Varga Z, Schubert AR, Asaro AB, Silva JR. The Xenopus Oocyte Cut-open Vaseline Gap Voltage-clamp Technique With Fluorometry. J Vis Exp. 2014;:51040. doi:10.3791/51040. PMID:24637712

[19] Sakmann B, Neher E. (eds). Single-channel recording. Plenum Press, New York, 1995. doi:10.1002/0471142301.ns0608s02. PMID:18428518.

[20] Williams SR, Wozny C. Errors in the measurement of voltage-activated ion channels in cell-attached patch-clamp recordings. Nat Comm. 2011;2:242.

[21] Catterall WA. Ion channel voltage sensors: structure, function, and pathophysiology. Neuron. 2010;67:915-28. doi:10.1016/j.neuron.2010.08.021. PMID:20869590

[22] Goldin AL, Barchi RL, Caldwell JH, Hofmann F, Howe JR, Hunter JC, Kallen RG, Mandel G, Meisler MH, Netter YB, et al. Nomenclature of Voltage-Gated Sodium Channels. Neuron. 2000;28:365-8. doi:10.1016/S0896-6273(00)00116-1. PMID:11144347

[23] Cormier JW, Rivolta I, Tateyama M, Yang A-S, Kass RS. Secondary structure of the human cardiac Na+ channel C terminus: evidence for a role of helical structures in modulation of channel inactivation. J Biol Chem. 2002;277:9233-41. doi:10.1074/jbc.M110204200. PMID:11741959

[24] Chagot B, Potet F, Balser JR, Chazin WJ. Solution NMR structure of the C-terminal EF-hand domain of human cardiac sodium channel NaV1.5. J Biol Chem. 2009;284:6436-45. doi:10.1074/jbc.M807747200. PMID:19074138

[25] Armstrong CM, Bezanilla F, Rojas E. Destruction of Sodium Conductance Inactivation in Squid Axons Perfused with Pronase. J Gen Physiol. 1973;62:375 LP-391. doi:10.1085/jgp.62.4.375. PMID:4755846

[26] Vassilev PM, Scheuer T, Catterall WA. Identification of an intracellular peptide segment involved in sodium channel inactivation. Science. 1988;241:1658-61. doi:10.1126/science.2458625. PMID:2458625

[27] Stuhmer W, Conti F, Suzuki H, Wang X, Noda M, Yahagi N, Kubo H, Numa S. Structural parts involved in activation

and inactivation of the sodium channel. Nature. 1989;339:597-603. doi:10.1038/339597a0. PMID:2543931

[28] Patton DE, Goldin AL. A voltage-dependent gating transition induces use-dependent block by tetrodotoxin of rat IIA sodium channels expressed in Xenopus oocytes. Neuron. 1991;7:637-47. doi:10.1016/0896-6273(91)90376-B. PMID:1657057

[29] West JW, Patton DE, Scheuer T, Wang Y, Goldin AL, Catterall WA. A cluster of hydrophobic amino acid residues required for fast Na(+)-channel inactivation. Proc Natl Acad Sci U S A. 1992;89:10910-4. doi:10.1073/pnas.89.22.10910. PMID:1332060

[30] Kellenberger S, West JW, Scheuer T, Catterall WA. Molecular Analysis of the Putative Inactivation Particle in the Inactivation Gate of Brain Type IIA Na+ Channels. J Gen Physiol. 1997;109:589-605. doi:10.1085/jgp.109.5.589. PMID:9154906

[31] Rohl CA, Boeckman FA, Baker C, Scheuer T, Catterall WA, Klevit RE. Solution structure of the sodium channel inactivation gate. Biochemistry. 1999;38:855-61. doi:10.1021/bi9823380. PMID:9893979

[32] Kellenberger S, Scheuer T, Catterall WA. Movement of the Na+ channel inactivation gate during inactivation. J Biol Chem. 1996;271:30971-9. doi:10.1074/jbc.271.48.30971. PMID:8940085

[33] Kellenberger S, West JW, Catterall WA, Scheuer T. Molecular analysis of potential hinge residues in the inactivation gate of brain type IIA Na+ channels. J Gen Physiol. 1997;109:607-17. doi:10.1085/jgp.109.5.607. PMID:9154907

[34] Bezanilla F. How membrane proteins sense voltage. Nat Rev Mol Cell Biol. 2008;9:323-32. doi:10.1038/nrm2376. PMID:18354422

[35] Armstrong CM, Bezanilla F. Inactivation of the sodium channel. II. Gating current experiments. J Gen Physiol. 1977;70:567-90. PMID:591912.doi:10.1085/jgp.70.5.567

[36] Mannuzzu LM, Moronne MM, Isacoff EY. Direct physical measure of conformational rearrangement underlying potassium channel gating. Science (80-). 1996;271:213. PMID:8539623.doi:10.1126/science.271.5246.213

[37] Cha A, Ruben PC, George ALJ, Fujimoto E, Bezanilla F. Voltage sensors in domains III and IV, but not I and II, are immobilized by Na+ channel fast inactivation. Neuron. 1999;22:73-87. doi:10.1016/S0896-6273(00)80680-7. PMID:10027291

[38] Smith MR, Goldin AL. Interaction between the sodium channel inactivation linker and domain III S4-S5. Biophys J. 1997;73:1885-95. doi:10.1016/S0006-3495(97)78219-5. PMID:9336184

[39] Smits JPP, Veldkamp MW, Bezzina CR, Bhuiyan ZA, Wedekind H, Schulze-Bahr E, Wilde AAM. Substitution of a conserved alanine in the domain IIIS4–S5 linker of the cardiac sodium channel causes long QT syndrome. Cardiovasc Res. 2005;67:459-66. doi:10.1016/j.cardiores.2005.01.017. PMID:16039271

[40] Lerche H, Peter W, Fleischhauer R, Pika-Hartlaub U, Malina T, Mitrovic N, Lehmann-Horn F. Role in fast inactivation of the IV/S4-S5 loop of the human muscle Na+ channel probed by cysteine mutagenesis. J Physiol. 1997;505:345-52. doi:10.1111/j.1469-7793.1997.345bb.x. PMID:9423178

[41] McPhee JC, Ragsdale DS, Scheuer T, Catterall WA. A critical role for the S4-S5 intracellular loop in domain IV of the sodium channel alpha-subunit in fast inactivation. J Biol Chem. 1998;273:1121-9. doi:10.1074/jbc.273.2.1121. PMID:9422778

[42] Popa MO, Alekov AK, Bail S, Lehmann-Horn F, Lerche H. Cooperative effect of S4-S5 loops in domains D3 and D4 on fast inactivation of the Na+ channel. J Physiol. 2004;561:39-51. doi:10.1113/jphysiol.2004.065912. PMID:15459238

[43] McPhee JC, Ragsdale DS, Scheuer T, Catterall WA. A critical role for transmembrane segment IVS6 of the sodium channel alpha subunit in fast inactivation. J Biol Chem. 1995;270:12025-34. doi:10.1074/jbc.270.20.12025. PMID:7744852

[44] McPhee JC, Ragsdale DS, Scheuer T, Catterall WA. A mutation in segment IVS6 disrupts fast inactivation of sodium channels. Proc Natl Acad Sci U S A. 1994;91:12346-50. doi:10.1073/pnas.91.25.12346. PMID:7991630

[45] Yarov-Yarovoy V, McPhee JC, Idsvoog D, Pate C, Scheuer T, Catterall WA. Role of Amino Acid Residues in Transmembrane Segments IS6 and IIS6 of the Na+ Channel α Subunit in Voltage-dependent Gating and Drug Block. J Biol Chem. 2002;277:35393-401. doi:10.1074/jbc.M206126200. PMID:12130650

[46] Yarov-Yarovoy V, Brown J, Sharp EM, Clare JJ, Scheuer T, Catterall WA. Molecular determinants of voltage-dependent gating and binding of pore-blocking drugs in transmembrane segment IIIS6 of the Na(+) channel alpha subunit. J Biol Chem. 2001;276:20-7. doi:10.1074/jbc.M006992200. PMID:11024055

[47] Wang S-Y, Bonner K, Russell C, Wang GK. Tryptophan Scanning of D1S6 and D4S6 C-Termini in Voltage-Gated Sodium Channels. Biophys J. 2003;85:911-20. doi:10.1016/S0006-3495(03)74530-5. PMID:12885638

[48] Goldin AL. Mechanisms of sodium channel inactivation. Curr Opin Neurobiol. 2003;13:284-90. doi:10.1016/S0959-4388(03)00065-5. PMID:12850212

[49] Deschenes I, Trottier E, Chahine M. Implication of the C-terminal region of the alpha-subunit of voltage-gated sodium channels in fast inactivation. J Membr Biol. 2001;183:103-14. doi:10.1007/s00232-001-0058-5. PMID:11562792

[50] Mantegazza M, Yu FH, Catterall WA, Scheuer T. Role of the C-terminal domain in inactivation of brain and cardiac sodium channels. Proc Natl Acad Sci U S A. 2001;98:15348-53. doi:10.1073/pnas.211563298. PMID:11742069

[51] Wei J, Wang DW, Alings M, Fish F, Wathen M, Roden DM, George AL. Congenital Long-QT Syndrome Caused by a Novel Mutation in a Conserved Acidic Domain of the Cardiac Na+ Channel. Circulation.

1999;99:3165 LP-3171. doi:10.1161/01.CIR.99.24.3165. PMID:10377081

[52] Deschenes I, Baroudi G, Berthet M, Barde I, Chalvidan T, Denjoy I, Guicheney P, Chahine M. Electrophysiological characterization of SCN5A mutations causing long QT (E1784K) and Brugada (R1512W and R1432G) syndromes. Cardiovasc Res. 2000;46:55-65. doi:10.1016/S0008-6363(00)00006-7. PMID:10727653

[53] Motoike HK, Liu H, Glaaser IW, Yang A-S, Tateyama M, Kass RS. The Na+ channel inactivation gate is a molecular complex: a novel role of the COOH-terminal domain. J Gen Physiol. 2004;123:155-65. doi:10.1085/jgp.200308929. PMID:14744988

[54] Goldschen-Ohm MP, Capes DL, Oelstrom KM, Chanda B. Multiple pore conformations driven by asynchronous movements of voltage sensors in a eukaryotic sodium channel. Nat Commun. 2013;4:1350. doi:10.1038/ncomms2356. PMID:23322038

[55] Silva JR, Goldstein SAN. Voltage-sensor movements describe slow inactivation of voltage-gated sodium channels I: Wild-type skeletal muscle Na(V)1.4. J Gen Physiol. 2013;141:309-21. doi:10.1085/jgp.201210909. PMID:23401571

[56] Silva JR, Goldstein SAN. Voltage-sensor movements describe slow inactivation of voltage-gated sodium channels II: A periodic paralysis mutation in NaV1.4 (L689I). J Gen Physiol. 2013;141:323 LP-334. doi:10.1085/jgp.201210910

[57] Hsu EJ, Zhu W, Schubert AR, Voelker T, Varga Z, Silva JR. Regulation of Na+ channel inactivation by the DIII and DIV voltage-sensing domains. J Gen Physiol. 2017;14:389-403. doi:10.1085/jgp.201611678. PMID:28232510.

[58] Varga Z, Zhu W, Schubert AR, Pardieck JL, Krumholz A, Hsu EJ, Zaydman MA, Cui J, Silva JR. Direct Measurement of Cardiac Na+ Channel Conformations Reveals Molecular Pathologies of Inherited Mutations. Circ Arrhythmia Electrophysiol. 2015;8:1228-39. doi:10.1161/CIRCEP.115.003155

[59] Hartshorne RP, Catterall WA. The sodium channel from rat brain. Purification and subunit composition. J Biol Chem. 1984;259:1667-75. PMID:6319405

[60] Kazen-Gillespie KA, Ragsdale DS, D'Andrea MR, Mattei LN, Rogers KE, Isom LL. Cloning, Localization, and Functional Expression of Sodium Channel β1A Subunits. J Biol Chem.. 2000;275:1079-88. doi:10.1074/jbc.275.2.1079

[61] Messner DJ, Catterall WA. The sodium channel from rat brain. Separation and characterization of subunits. J Biol Chem. 1985;260:10597-604. PMID:2411726

[62] Morgan K, Stevens EB, Shah B, Cox PJ, Dixon AK, Lee K, Pinnock RD, Hughes J, Richardson PJ, Mizuguchi K, et al. beta 3: an additional auxiliary subunit of the voltage-sensitive sodium channel that modulates channel gating with distinct kinetics. Proc Natl Acad Sci U S A. 2000;97:2308-13. doi:10.1073/pnas.030362197. PMID:10688874

[63] Yu FH, Westenbroek RE, Silos-Santiago I, McCormick KA, Lawson D, Ge P, Ferriera H, Lilly J, DiStefano PS, Catterall WA, et al. Sodium channel beta4, a new disulfide-linked auxiliary subunit with similarity to beta2. J Neurosci. 2003;23:7577-85. PMID:12930796

[64] Calhoun JD, Isom LL. The role of non-pore-forming beta subunits in physiology and pathophysiology of voltage-gated sodium channels. Handb Exp Pharmacol. 2014;221:51-89. doi:10.1007/978-3-642-41588-3_4. PMID:24737232

[65] Bao Y, Isom LL. NaV1.5 and Regulatory β Subunits in Cardiac Sodium Channelopathies. Card Electrophysiol Clin. 2014;6:679-94. doi:10.1016/j.ccep.2014.07.002

[66] Isom LL, De Jongh KS, Patton DE, Reber BF, Offord J, Charbonneau H, Walsh K, Goldin AL, Catterall WA. Primary structure and functional expression of the beta 1 subunit of the rat brain sodium channel. Science. 1992;256:839-42. doi:10.1126/science.1375395. PMID:1375395

[67] Das S, Gilchrist J, Bosmans F, Van Petegem F. Binary architecture of the Nav1.2-beta2 signaling complex. Elife. 2016; 170 (470-482); e.11. doi:10.7554/eLife.10960. PMID:26894959.

[68] O'Malley HA, Isom LL. Sodium channel beta subunits: emerging targets in channelopathies. Annu Rev Physiol. 2015;77:481-504. doi:10.1146/annurev-physiol-021014-071846. PMID:25668026

[69] Dominguez JN, Navarro F, Franco D, Thompson RP, Aranega AE. Temporal and spatial expression pattern of beta1 sodium channel subunit during heart development. Cardiovasc Res. 2005;65:842-50. doi:10.1016/j.cardiores.2004.11.028. PMID:15721864

[70] Okata S, Yuasa S, Suzuki T, Ito S, Makita N, Yoshida T, Li M, Kurokawa J, Seki T, Egashira T, et al. Embryonic type Na+ channel β-subunit, SCN3B masks the disease phenotype of Brugada syndrome.. 2016;6:34198. PMID:27677334 doi:10.1038/srep34198

[71] Malhotra JD, Kazen-Gillespie K, Hortsch M, Isom LL. Sodium channel beta subunits mediate homophilic cell adhesion and recruit ankyrin to points of cell-cell contact. J Biol Chem. 2000;275:11383-8. doi:10.1074/jbc.275.15.11383. PMID:10753953

[72] Isom LL, Ragsdale DS, De Jongh KS, Westenbroek RE, Reber BF, Scheuer T, Catterall WA. Structure and function of the beta 2 subunit of brain sodium channels, a transmembrane glycoprotein with a CAM motif. Cell. 1995;83:433-42. doi:10.1016/0092-8674(95)90121-3. PMID:8521473

[73] Fahmi AI, Patel M, Stevens EB, Fowden AL, John JE, Lee K, Pinnock R, Morgan K, Jackson AP, Vandenberg JI. The sodium channel beta-subunit SCN3b modulates the kinetics of SCN5a and is expressed heterogeneously in sheep heart. J Physiol. 2001;537:693-700. doi:10.1113/jphysiol.2001.012691. PMID:11744748

[74] Watanabe H, Darbar D, Kaiser DW, Jiramongkolchai K, Chopra S, Donahue BS, Kannankeril PJ, Roden DM. Mutations in sodium channel beta1- and beta2-subunits

associated with atrial fibrillation. Circ Arrhythm Electrophysiol. 2009;2:268-75. doi:10.1161/CIRCEP.108.779181. PMID:19808477

[75] Yan Z, Zhou Q, Wang L, Wu J, Zhao Y, Huang G, Peng W, Shen H, Lei J, Yan N. Structure of the Nav1.4-β1 Complex from Electric Eel. Cell. 2017; doi:10.1016/j.cell.2017.06.039.

[76] Zhu W, Voelker TL, Varga Z, Schubert AR, Nerbonne JM, Silva JR. Mechanisms of noncovalent β subunit regulation of Na+ channel gating. J Gen Physiol. 2017; doi:10.1085/jgp.201711802

[77] Wilde AAM, Brugada R. Phenotypical Manifestations of Mutations in the Genes Encoding Subunits of the Cardiac Sodium Channel. Circ Res. 2011;108:884 LP-897. doi:10.1161/CIRCRESAHA.110.238469

[78] Abriel H. Cardiac sodium channel Na(v)1.5 and interacting proteins: Physiology and pathophysiology. J Mol Cell Cardiol. 2010;48:2-11. doi:10.1016/j.yjmcc.2009.08.025. PMID:19744495

[79] Meregalli PG, Wilde AAM, Tan HL. Pathophysiological mechanisms of Brugada syndrome: Depolarization disorder, repolarization disorder, or more? Cardiovasc Res. 2005;67:367-78. doi:10.1016/j.cardiores.2005.03.005. PMID:15913579

[80] Giudicessi JR, Ackerman MJ. Genotype- and phenotype-guided management of congenital long QT syndrome. Curr Probl Cardiol. 2013;38:417-55. doi:10.1016/j.cpcardiol.2013.08.001. PMID:24093767

[81] Lopez-Santiago LF, Meadows LS, Ernst SJ, Chen C, Malhotra JD, McEwen DP, Speelman A, Noebels JL, Maier SKG, Lopatin AN, et al. Sodium channel Scn1b null mice exhibit prolonged QT and RR intervals. J Mol Cell Cardiol. 2007;43:636-47. doi:10.1016/j.yjmcc.2007.07.062. PMID:17884088

[82] Bao Y, Willis BC, Frasier CR, Lopez-Santiago LF, Lin X, Ramos-Mondragón R, Auerbach DS, Chen C, Wang Z, Anumonwo J, et al. Scn2b Deletion in Mice Results in Ventricular and Atrial Arrhythmias. Circ Arrhythmia Electrophysiol. 2016;9. doi:10.1161/CIRCEP.116.003923

[83] Hakim, P, Gurung P, Pedersen P, Thresher P, Brice P, Lawrence P. Scn3b knockout mice exhibit abnormal ventricular electrophysiological properties. Prog Biophys Mol Biol. 2008;98:251-66. doi:10.1016/j.pbiomolbio.2009.01.005. PMID:19351516

[84] Hakim, P., Thresher, R., Grace, A.A. HCL. Effects of flecainide and quinidine on action potential and ventricular arrhythmogenic properties in Scn3b knockout mice. Clin Exp Pharmacol Physiol. 2010;37:782-9. doi:10.1111/j.1440-1681.2010.05369.x PMID:20132234

[85] Mori M, Konno T, Ozawa T, Murata M, Imoto K, Nagayama K. Novel interaction of the voltage-dependent sodium channel (VDSC) with calmodulin: does VDSC acquire calmodulin-mediated Ca2+-sensitivity? Biochemistry. 2000;39:1316-23. doi:10.1021/bi9912600. PMID:10684611

[86] Klee CB, Crouch TH, Richman PG. Calmodulin. Annu Rev Biochem. 1980;49:489-515. doi:10.1146/annurev.bi.49.070180.002421. PMID:6250447

[87] Van Petegem F, Lobo PA, Ahern CA. Seeing the forest through the trees: towards a unified view on physiological calcium regulation of voltage-gated sodium channels. Biophys J. 2012;103:2243-51. doi:10.1016/j.bpj.2012.10.020. PMID:23283222

[88] Deschenes I, Neyroud N, DiSilvestre D, Marban E, Yue DT, Tomaselli GF. Isoform-specific modulation of voltage-gated Na(+) channels by calmodulin. Circ Res. 2002;90:E49-57. doi:10.1161/01.RES.0000012502.92751.E6. PMID:11884381

[89] Tan HL, Kupershmidt S, Zhang R, Stepanovic S, Roden DM, Wilde AAM, Anderson ME, Balser JR. A calcium sensor in the sodium channel modulates cardiac excitability. Nature. 2002;415:442-7. doi:10.1038/415442a. PMID:11807557

[90] Casini S, Verkerk AO, van Borren MMGJ, van Ginneken ACG, Veldkamp MW, de Bakker JMT, Tan HL. Intracellular calcium modulation of voltage-gated sodium channels in ventricular myocytes. Cardiovasc Res. 2009;81:72-81. doi:10.1093/cvr/cvn274. PMID:18829699

[91] Ben-Johny M, Yang PS, Niu J, Yang W, Joshi-Mukherjee R, Yue DT. Conservation of Ca2+/calmodulin regulation across Na and Ca2+ channels. Cell. 2014;157:1657-70. doi:10.1016/j.cell.2014.04.035. PMID:24949975

[92] Wingo TL, Shah VN, Anderson ME, Lybrand TP, Chazin WJ, Balser JR. An EF-hand in the sodium channel couples intracellular calcium to cardiac excitability. Nat Struct Mol Biol. 2004;11:219-25. doi:10.1038/nsmb737. PMID:14981509

[93] Biswas S, Deschenes I, Disilvestre D, Tian Y, Halperin VL, Tomaselli GF. Calmodulin regulation of Nav1.4 current: role of binding to the carboxyl terminus. J Gen Physiol. 2008;131:197-209. doi:10.1085/jgp.200709863. PMID:18270170

[94] Sarhan MF, Van Petegem F, Ahern CA. A double tyrosine motif in the cardiac sodium channel domain III-IV linker couples calcium-dependent calmodulin binding to inactivation gating. J Biol Chem. 2009;284:33265-74. doi:10.1074/jbc.M109.052910. PMID:19808664

[95] Sarhan MF, Tung C-C, Van Petegem F, Ahern CA. Crystallographic basis for calcium regulation of sodium channels. Proc Natl Acad Sci U S A. 2012;109:3558-63. doi:10.1073/pnas.1114748109. PMID:22331908

[96] Wang C, Chung BC, Yan H, Lee S-Y, Pitt GS. Crystal structure of the ternary complex of a NaV C-terminal domain, a fibroblast growth factor homologous factor, and calmodulin. Structure. 2012;20:1167-76. doi:10.1016/j.str.2012.05.001. PMID:22705208

[97] Wang C, Chung BC, Yan H, Wang H-G, Lee S-Y, Pitt GS. Structural analyses of Ca(2)(+)/CaM interaction with NaV channel C-termini reveal mechanisms of calcium-dependent regulation. Nat Commun. 2014;5:4896. doi:10.1038/ncomms5896. PMID:25232683

[98] Hennessey JA, Wei EQ, Pitt GS. Fibroblast Growth Factor Homologous Factors Modulate Cardiac Calcium Channels. Circ Res. 2013;113: doi:10.1161/CIRCRESAHA.113.301215. PMID:23804213

[99] Liu C, Dib-Hajj SD, Renganathan M, Cummins TR, Waxman SG. Modulation of the cardiac sodium channel Nav1.5 by fibroblast growth factor homologous factor 1B. J Biol Chem. 2003;278:1029-36. doi:10.1074/jbc.M207074200. PMID:12401812

[100] Musa H, Kline CF, Sturm AC, Murphy N, Adelman S, Wang C, Yan H, Johnson BL, Csepe TA, Kilic A, et al. SCN5A variant that blocks fibroblast growth factor homologous factor regulation causes human arrhythmia. Proc Natl Acad Sci. 2015;112:12528-33. doi:10.1073/pnas.1516430112. PMID:26392562

[101] Jones DK, Peters CH, Tolhurst SA, Claydon TW, Ruben PC. Extracellular proton modulation of the cardiac voltage-gated sodium channel, NaV1.5. Biophys J. 2011;101:2147-56. doi:10.1016/j.bpj.2011.08.056. PMID:22067152

[102] Vilin YY, Peters CH, Ruben PC. Acidosis differentially modulates inactivation in Nav1.2, Nav1.4, and Nav1.5 channels. Front Pharmacol. 2012;3:109. doi:10.3389/fphar.2012.00109. PMID:22701426

[103] Peters CH, Abdelsayed M, Ruben PC. Triggers for arrhythmogenesis in the Brugada and long QT 3 syndromes. Prog Biophys Mol Biol. 2016;120:77-88. doi:10.1016/j.pbiomolbio.2015.12.009. PMID:26713557

[104] Jones DK, Claydon TW, Ruben PC. Extracellular protons inhibit charge immobilization in the cardiac voltage-gated sodium channel. Biophys J. 2013;105:101-7. doi:10.1016/j.bpj.2013.04.022. PMID:23823228

[105] Jones DK, Peters CH, Allard CR, Claydon TW, Ruben PC. Proton sensors in the pore domain of the cardiac voltage-gated sodium channel. J Biol Chem. 2013;288:4782-91. doi:10.1074/jbc.M112.434266. PMID:23283979

[106] Jones DK, Ruben PC. Proton modulation of cardiac I Na: A potential arrhythmogenic trigger. Handb Exp Pharmacol. 2014;221:169-81. doi:10.1007/978-3-642-41588-3_8. PMID:24737236

[107] Omar HR, El-Khabiry E, Dalvi P, Mangar D, Camporesi EM. Brugada ECG pattern during hyperkalemic diabetic ketoacidosis. Ther Adv Endocrinol Metab. 2017;8:20-1. doi:10.1177/2042018816680589. PMID:28203362

[108] Anselm DD, Evans JM, Baranchuk A. Brugada phenocopy: A new electrocardiogram phenomenon. World J Cardiol. 2014;6:81-6. doi:10.4330/wjc.v6.i3.81. PMID:24669289

[109] Peters CH, Ruben PC. Acidosis: A Possible Trigger for Brugada Syndrome Associated Arrhythmia. Biophys J. 2014;106:327a. doi:10.1016/j.bpj.2013.11.1880

[110] Peters CH, Abdelsayed M, Ruben PC. Triggers for arrhythmogenesis in the Brugada and long QT 3 syndromes. Prog Biophys Mol Biol. 2016;120:77-88. doi:10.1016/j.pbiomolbio.2015.12.009. PMID:26713557

[111] Hu RM, Tan BH, Tester DJ, Song C, He Y, Dovat S, Peterson BZ, Ackerman MJ, Makielski JC. Arrhythmogenic biophysical phenotype for SCN5A mutation S1787N depends upon splice variant background and intracellular acidosis. PLoS One. 2015;10:e0124921. doi:10.1371/journal.pone.0124921. PMID:25923670

[112] Knowlton FP, Starling EH. The influence of variations in temperature and blood-pressure on the performance of the isolated mammalian heart. J Physiol. 1912;44:206-19. doi:10.1113/jphysiol.1912.sp001511. PMID:16993122

[113] Pasquié JL, Sanders P, Hocini M, Hsu LF, Scavée C, Jais P, Takahashi Y, Rotter M, Sacher F, Victor J, et al. Fever as a precipitant of idiopathic ventricular fibrillation in patients with normal hearts. J Cardiovasc Electrophysiol. 2004;15:1271-6. doi:10.1046/j.1540-8167.2004.04388.x. PMID:15574177

[114] Abdelsayed M, Peters CH, Ruben PC. Differential thermosensitivity in mixed syndrome cardiac sodium channel mutants. J Physiol. 2015;593:4201-23. doi:10.1113/JP270139. PMID:26131924

[115] Dumaine R, Towbin JA, Brugada P, Vatta M, Nesterenko D V., Nesterenko V V., Brugada J, Brugada R, Antzelevitch C. Ionic Mechanisms Responsible for the Electrocardiographic Phenotype of the Brugada Syndrome Are Temperature Dependent. Circ Res. 1999;85:803-9. doi:10.1161/01.RES.85.9.803. PMID:10532948

[116] Keller DI, Rougier JS, Kucera JP, Benammar N, Fressart V, Guicheney P, Madle A, Fromer M, Schläpfer J, Abriel H. Brugada syndrome and fever: Genetic and molecular characterization of patients carrying SCN5A mutations. Cardiovasc Res. 2005;67:510-9. doi:10.1016/j.cardiores.2005.03.024. PMID:15890323

[117] Adler A, Topaz G, Heller K, Zeltser D, Ohayon T, Rozovski U, Halkin A, Rosso R, Ben-Shachar S, Antzelevitch C, et al. Fever-induced Brugada pattern: How common is it and what does it mean? Hear Rhythm. 2013;10:1375-82. doi:10.1016/j.hrthm.2013.07.030. PMID:23872691

[118] De Marco S, Giannini C, Chiavaroli V, De Leonibus C, Chiarelli F, Mohn A. Brugada syndrome unmasked by febrile illness in an asymptomatic child. J. Pediatr.2012;161:769-769.e1. doi:10.1016/j.jpeds.2012.04.034. PMID:22608909

[119] Rijal J, Giri S, Khanal S, Dahal K. A case of Brugada Syndrome unmasked by a postoperative febrile state. Casp J Intern Med. 2015;6:43-5. PMID:26221497

[120] Gima K, Rudy Y. Ionic current basis of electrocardiographic waveforms: A model study. Circ Res. 2002;90:889-96. doi:10.1161/01.RES.0000016960.61087.86. PMID:11988490

[121] Schoorlemmer J, Goldfarb M. Fibroblast growth factor homologous factors are intracellular signaling proteins. Curr Biol. 2001;11:793-7. doi:10.1016/S0960-9822(01)00232-9. PMID:11378392

[122] Park DS, Shekhar A, Marra C, Lin X, Vasquez C, Solinas S, Kelley K, Morley G, Goldfarb M, Fishman GI. Fhf2 gene deletion causes temperature-sensitive cardiac conduction failure. Nat Commun. 2016;7:12966. doi:10.1038/ncomms12966. PMID:27701382

[123] Ahern CA, Payandeh J, Bosmans F, Chanda B. The hitchhiker's guide to the voltage-gated sodium channel galaxy. J Gen Physiol. 2016;147:1-24. doi:10.1085/jgp.201511492. PMID:26712848

[124] Bezanilla F, Armstrong CM. Inactivation of the sodium channel. I. Sodium current experiments. J

Gen Physiol. 1977;70:549-66. doi:10.1085/jgp.70.5.549. PMID:591911

[125] Colquhoun D, Hawkes AG. Relaxation and Fluctuations of Membrane Currents that Flow through Drug-Operated Channels. Proc R Soc London Ser B Biol Sci. 1977;199:231 LP-262. doi:10.1098/rspb.1977.0137

[126] Colquhoun D, Hawkes AG. On the stochastic properties of single ion channels. Proc R Soc London Ser B, Biol Sci. 1981;211:205-35. doi:10.1098/rspb.1981.0003. PMID:6111797

[127] Horn R, Lange K. Estimating kinetic constants from single channel data. Biophys J. 1983;43:207-23. doi:10.1016/S0006-3495(83)84341-0. PMID:6311301

[128] Rudy Y, Silva JR. Computational biology in the study of cardiac ion channels and cell electrophysiology. Q Rev Biophys. 2006;39:57-116. doi:10.1017/S0033583506004227. PMID:16848931

[129] Vandenberg CA, Bezanilla F. A sodium channel gating model based on single channel, macroscopic ionic, and gating currents in the squid giant axon. Biophys J. 1991;60:1511-33. doi:10.1016/S0006-3495(91)82186-5. PMID:1663796

[130] Keynes RD. A New Look at the Mechanism of Activation and Inactivation of Voltage-Gated Ion Channels. Proc R Soc London Ser B Biol Sci. 1992;249:107 LP-112. doi:10.1098/rspb.1992.0091

[131] Chanda B, Bezanilla F. Tracking Voltage-dependent Conformational Changes in Skeletal Muscle Sodium Channel during Activation. J Gen Physiol. 2002;120:629 LP-645. doi:10.1085/jgp.20028679. PMID:12407076

[132] Correa AM, Bezanilla F. Gating of the squid sodium channel at positive potentials: II. Single channels reveal two open states. Biophys J. 1994;66:1864-78. doi:10.1016/S0006-3495(94)80979-8. PMID:8075323

[133] Keynes RD, Elinder F. Modelling the activation, opening, inactivation and reopening of the voltage-gated sodium channel. Proc R Soc B Biol Sci. 1998;265:263-70. doi:10.1098/rspb.1998.0291. PMID:9523428

[134] Clancy CE, Rudy Y. Linking a genetic defect to its cellular phenotype in a cardiac arrhythmia. Nature. 1999;400:566-9. doi:10.1038/23034. PMID:10448858

[135] Szendroedi J, Sandtner W, Zarrabi T, Zebedin E, Hilber K, Dudley SCJ, Fozzard HA, Todt H. Speeding the recovery from ultraslow inactivation of voltage-gated Na+ channels by metal ion binding to the selectivity filter: a foot-on-the-door? Biophys J. 2007;93:4209-24. doi:10.1529/biophysj.107.104794. PMID:17720727

[136] Menon V, Spruston N, Kath WL. A state-mutating genetic algorithm to design ion-channel models. Proc Natl Acad Sci U S A. 2009;106:16829-34. doi:10.1073/pnas.0903766106. PMID:19805381

[137] Teed ZR, Silva JR. A computationally efficient algorithm for fitting ion channel parameters. MethodsX. 2016;3:577-88. doi:10.1016/j.mex.2016.11.001. PMID:27924282

[138] Silva JR, Pan H, Wu D, Nekouzadeh A, Decker KF, Cui J, Baker NA, Sept D, Rudy Y. A multiscale model linking ion-channel molecular dynamics and electrostatics to the cardiac action potential. Proc Natl Acad Sci. 2009;106:11102-6. doi:10.1073/pnas.0904505106. PMID:19549851

[139] Shen H, Zhou Q, Pan X, Li Z, Wu J, Yan N. Structure of a eukaryotic voltage-gated sodium channel at near-atomic resolution. Science. 2017;355. doi:10.1126/science.aal4326. PMID:28183995

[140] Zhu W, Varga Z, Silva JR. Molecular motions that shape the cardiac action potential: Insights from voltage clamp fluorometry. Prog Biophys Mol Biol. 2016;120:3-17. doi:10.1016/j.pbiomolbio.2015.12.003. PMID:26724572

[141] Brettmann JB, Urusova D, Tonelli M, Silva JR, Henzler-Wildman KA. Role of protein dynamics in ion selectivity and allosteric coupling in the NaK channel. Proc Natl Acad Sci. 2015;112:15366-71. doi:10.1073/pnas.1515965112. PMID:26621745

[142] Kleber AG, Rudy Y. Basic mechanisms of cardiac impulse propagation and associated arrhythmias. Physiol Rev. 2004;84:431-88. doi:10.1152/physrev.00025.2003. PMID:15044680